Self-Recognition and Self-Assembly of Folic Acid Salts: Columnar Liquid Crystalline Polymorphism and the Column Growth Process

Federica Ciuchi,[‡] Giovanni Di Nicola,[‡] Hermann Franz,[‡,§] Giovanni Gottarelli,*[,†] Paolo Mariani,*[,‡] Maria Grazia Ponzi Bossi,[‡] and Gian Piero Spada*[,†]

Contribution from the Dipartimento di Chimica Organica "A. Mangini", Università di Bologna, Via S. Donato, 15, I-40127 Bologna, Italy, and Istituto di Scienze Fisiche, Università di Ancona, Via Ranieri, 65, I-60131 Ancona, Italy

Received March 7, 1994[⊕]

Abstract: Alkaline folates in water, with or without added NaCl, form columnar mesophases; the columns are composed of a stacked array of folate tetramers held together by Hoogsteen-type hydrogen bonds and stacking interactions. There is a considerable difference in both the liquid crystalline polymorphism and the columnar characteristics in pure water and those in 1 mol L^{-1} NaCl solutions. In pure water, the tetramer–tetramer interaction is weak, the columnar length changes slowly with the folate concentration, and only the hexagonal mesophase is observed. In 1 mol L^{-1} NaCl, the tetramer–tetramer interaction is stronger, a cholesteric mesophase is observed, and, even at relatively low folate concentration, the length of the columns is significant (*ca.* 20 disks at the isotropic-to-cholesteric transition). In both cases, the columns are finite at all concentrations investigated. The formation of a cholesteric mesophase with a pitch of *ca.* 14 μm indicates that the tetramers do not pile up in register but are rotated one with respect to the other to give a chiral column similar both to the four-stranded helix of poly(G) and to the columnar aggregates formed by homoguanylic oligodeoxynucleotides.

Introduction

Self-assembly and self-organization have been reported for both organic and inorganic molecules.[1] The property of biological molecules to self-associate in water is of particular interest;[1a] in some cases, this may lead to liquid crystalline phases.[2] Columnar mesophases obtained from deoxyguanosine derivatives have been described,[3-7] and their structure is now well-known: the columns are composed of stacked arrays of tetramers, each formed by four Hoogsteen-bonded[8] guanosine residues. This tetrameric structure was recently found to play an important role in telomeres (the terminal part of chromosome), synthetic models of which have been investigated by several physicochemical techniques.[9] Structures with G-quartets were also found in a deoxynucleotide aptamer which inhibits trombin[10] as well as in phosphorotioate octanucleotides active against the human herpes simplex virus.[11] Folic acid is an important biologically active molecule characterized by the presence of the pterine heterocycle. In a preliminary communication, we have reported that also the salts of folic acid self-associate in water, leading to the formation of hexagonal columnar mesophases.[12] This behavior is related to the similarity between guanine and pterin moieties, which both possess a particular pattern of H-bond donor and acceptor groups leading to self-recognition and self-assembly (Figure 1).

In this paper, we report a detailed study of the self-assembly of alkaline folate to give liquid crystalline phases by X-ray diffraction, optical microscopy, and circular dichroism (CD) spectroscopy. The study of the assembly process in isotropic solutions by small angle neutron scattering (SANS), CD, and NMR will be described elsewhere.[13]

To our knowledge, in the literature there are no other reports on the self-assembly of folate; its possible biological significance has therefore never been considered. However, the first observation on the self-assembly of guanosine derivatives[14] was made about 80 years before the recognition of their biological significance.[15]

Phase Diagrams

Optical Microscopy and CD Results. The phase diagrams have been determined from the analysis of X-ray diffraction profiles recorded as a function of concentration and temperature and from polarizing optical microscopy observations. As already reported,[12] aqueous solutions of sodium and potassium salts of folic acid (Na_2Fol/H_2O and K_2Fol/H_2O), at room temperature

† Università di Bologna.
‡ Università di Ancona.
§ Present address: Physik Department E13, Technische Universitat Munchen, James Franck Strasse, 1, D-85748 Garching, Germany.
⊕ Abstract published in *Advance ACS Abstracts,* July 1, 1994.

(1) (a) Lehn, J.-M. *Angew. Chem., Int. Ed. Engl.* **1990**, *29*, 1304. (b) Krämer, R.; Lehn, J.-M.; Marquis-Rigault, A. *Proc. Natl. Acad. Sci. U.S.A.* **1993**, *90*, 5394.
(2) Hoffmann, S. *Z. Chem.* **1987**, *27*, 395.
(3) Mariani, P.; Mazabard, C.; Garbesi, A.; Spada, G. P. *J. Am. Chem. Soc.* **1989**, *111*, 6369–73.
(4) Spada, G. P.; Mariani, P.; Gottarelli, G.; Garbesi, A.; Bonazzi, S.; Ponzi Bossi, M. G.; De Morais, M. M.; Capobianco, M. *J. Am. Chem. Soc.* **1991**, *113*, 5809–16.
(5) Amaral, L. Q.; Itri, R.; Mariani, P.; Micheletto, R. *Liq. Cryst.* **1992**, *12*, 913.
(6) Mariani, P.; De Morais, M. M.; Gottarelli, G.; Spada, G. P.; Delacroix, H.; Tondelli, L. *Liq. Cryst.* **1993**, *15*, 757–78.
(7) Spada, G. P.; Carcuro, A.; Colonna, F. P.; Garbesi, A.; Gottarelli, G. *Liq. Cryst.* **1988**, *3*, 651–4.
(8) Hoogsteen, K. *Acta Crystallogr.* **1959**, *12*, 822–45.
(9) Zahler, A. M.; Williamson, J. R.; Cech, T. R.; Prescott, D. M. *Nature* **1991**, *350*, 718. Hardin, C. C.; Henderson, E.; Watson, T.; Prosser, J. K. *Biochemistry* **1991**, *30*, 4460. Balagurumoorthy, P.; Brahmachari, S. K.; Mohanty, D.; Bansal, M.; Sasisekharan, V. *Nucleic Acids Res.* **1992**, *20*, 4061. Lu, M.; Guo, Q.; Kallenbach, N. R. *Biochemistry* **1993**, *32*, 598. Wang, Y.; Patel, D. J. *Biochemistry* **1992**, *31*, 8112. Smith, F. W.; Feigon, J. *Nature* **1992**, *356*, 164. Kang, C.; Zhang, X.; Ratliff, R.; Moyzis, R.; Rich, A. *Nature* **1992**, *356*, 126. Gupta, G.; Garcia, A. E.; Guo, Q.; Lu, M.; Kallenbach, N. R. *Biochemistry* **1993**, *32*, 7098.
(10) Wang, K. Y.; McCurdy, S.; Shea, R. G.; Swaminathan, S.; Bolton, P. H. *Biochemistry* **1993**, *32*, 1899.
(11) Ecker, D. J.; Vickers, T. A.; Hanekak, R.; Driver, V.; Anderson, K. *Nucleic Acids Res.* **1993**, *21*, 1853.
(12) Bonazzi, S.; De Morais, M. M.; Gottarelli, G.; Mariani, P.; Spada, G. P. *Angew. Chem., Int. Ed. Engl.* **1993**, *32*, 248–50.
(13) Bonazzi, S.; Carsughi, F.; Di Nicola, G.; Gottarelli, G.; Mariani, P.; Mezzina, E.; Sabatucci, A.; Spada, G. P., manuscript in preparation.
(14) Bang, I. *Biochem. Zeitschr.* **1910**, *26*, 293.
(15) Sen, D.; Gilbert, W. *Nature* **1988**, *334*, 364. Kamenetskii, M. F. *Nature* **1989**, *342*, 737; **1992**, *356*, 105.

0002-7863/94/1516-7064$04.50/0

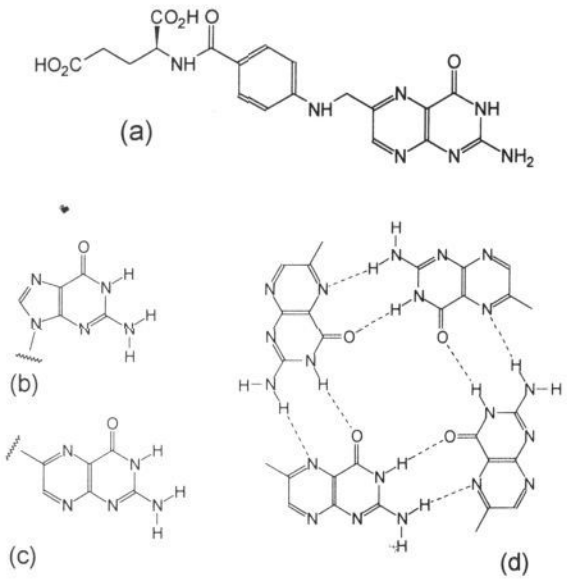

Figure 1. Folic acid structure (a) and the similarity between guanine (b) and pterin (c). As well as guanines, pterins also can self-recognize and generate Hoogsteen-bonded tetrads (d).

and above the critical concentration of about 0.35 w/w, become birefringent. The optical textures are typical of the hexagonal mesophases.

In the presence of 1 mol L^{-1} NaCl ($Na_2Fol/NaCl/H_2O$), the critical concentration at which the solution becomes liquid crystalline is lower, *ca.* 0.27 w/w, and two different mesophases can be detected: a cholesteric phase up to *ca.* 0.32 w/w and then a hexagonal phase. In Figure 2, the texture of the hexagonal phase is reported together with a microphotograph of a sample with a concentration gradient in which both textures coexist.

In the presence of 1 mol L^{-1} KCl ($K_2Fol/KCl/H_2O$), the situation is intermediate. In samples with a concentration gradient obtained by rapid evaporation of water, the typical cholesteric texture can be detected between the isotropic and the hexagonal phases at *ca.* 0.34 w/w, but we were not able to isolate a monophasic cholesteric system: in fact, if evaporation is slow, then the direct transition from the isotropic to the hexagonal phase, as for solutions of folate in water, is observed at *ca.* 0.34 w/w.

The cholesteric phase obtained from the $Na_2Fol/NaCl/H_2O$ system can easily be aligned by means of magnetic fields. If the field is parallel to the cell walls, then a "fingerprint" optical texture is obtained. In this texture, the cholesteric axis is parallel to the cell walls; this enables the determination of a pitch of 14 ± 1 μm for the cholesteric helix[16] by measuring the distance between two adjacent lines of equal extinction observed with a polarizing microscope (crossed polars). In general, the pitch depends on the concentration of the chiral solute,[7,17] but in this case, as a consequence of the small interval of existence of the phase (0.27–0.32 w/w), we were not able to verify this general trend. It should be noticed that the pitch is not unwound by the field. If the field is perpendicular to the cell walls, then a "planar" texture, in which also the helix axis is perpendicular to the cell walls, is obtained. This magnetic behavior indicates that the objects which compose the phase have negative diamagnetic anisotropy (type II cholesteric)[3,16] and supports the model proposed in which the pterin residues are perpendicular to the long axis of the rod: in fact, when the long axes of the aggregates are aligned perpendicularly to the magnetic field, the planes of pterins lie parallel to it, and this is the preferred orientation for an aromatic molecule.

(16) Yu, L. J.; Saupe, A. *J. Am. Chem. Soc.* **1980**, *102*, 4879.
(17) Robinson, C. *Tetrahedron* **1961**, *13*, 219–34.

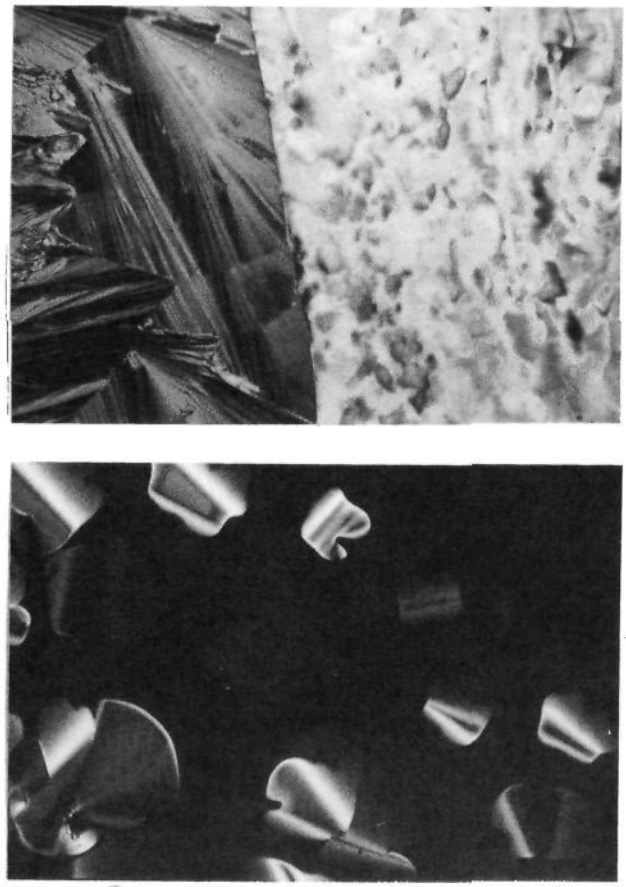

Figure 2. (Bottom) Star-domain texture, typical of a hexagonal phase, growing in the isotropic solution of Na_2Fol in water. (Top) Textures obtained by peripheral evaporation of a sample of the ternary system $Na_2Fol/NaCl/H_2O$ at the Chol → Hex transition: the higher concentration region (left side) displays the fan-shaped texture typical of the hexagonal mesophase, while the lower concentration region (right side) is cholesteric. Pictures were taken with crossed polars (original magnification 250×).

The handedness of the cholesteric phase can be deduced by circular dichroism (CD) spectroscopy.[4,18] In correspondence to the wavelength of the chromophoric absorption, a cholesteric phase with "planar" orientation exhibits a very intense CD signal, a few orders of magnitude greater than that given by the corresponding isotropic solution, due to the helical arrangement of the chromophoric groups. From the sign of this band, the handedness of the cholesteric phase may be inferred by eq 1, if information on the structure of the object forming the mesophase is available:[19]

$$(A_L - A_R)_j = p\nu_j^3 \Delta n (A_\parallel - A_\perp)_j / 2(\nu_j^2 - \nu_0^2) \qquad (1)$$

where $(A_L - A_R)_j$ is the CD at frequency ν_j, ν_0 is the frequency of the selective reflection which is related to the cholesteric pitch, Δn is the optical anisotropy, p is the pitch that is positive for a right-handed helix, and $(A_\parallel - A_\perp)_j$ is the linear dichroism of the helix-building object. In our case, we have a negative CD, indicating a left-handed cholesteric phase (although we do not have a detailed description of the pterin chromophore, it is well-known that allowed transitions in aromatic and heteroaromatic rings are in-plane polarized; hence, in analogy to DNA[20] and

(18) Gottarelli, G.; Spada, G. P. In *Circular Dichroism: Interpretations and Applications*; Nakanishi, K., Berova, N., Woody, R. W., Eds.; VCH: New York, 1994.
(19) Sackman, E.; Voss, J. *Chem. Phys. Lett.* **1972**, *14*, 528. Dudley, R. J.; Mason, S. F.; Peacock, R. D. *J. Chem. Soc., Perkin Trans. 2* **1975**, 997.

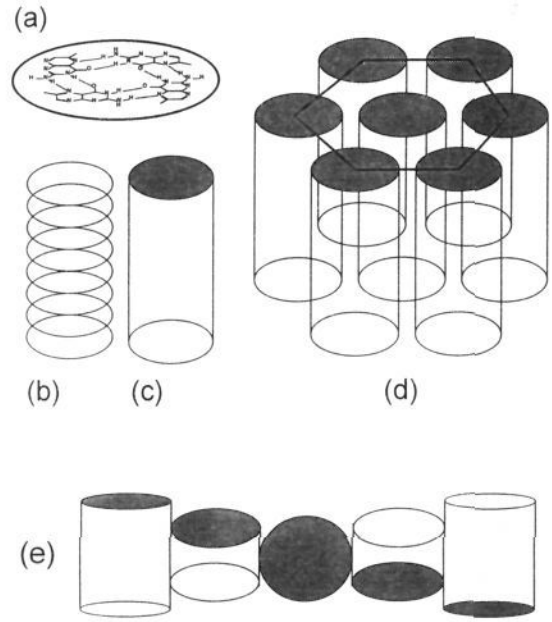

Figure 3. Model of formation of the columnar mesophases from folate. The tetramers of folate residues (a) pile up (b) to form columns (c). The columns can self-correlate to generate a mesophase with a hexagonal (d) or cholesteric (e) order.

guanosine tetraplex[4] systems, the linear dichroism and the optical anisotropy are likely to be negative).

The formation of a cholesteric mesophase with rather a short pitch (in the self-assembly of guanosine derivatives, pitches from 30 to 100 μm were observed)[4] is an indication that the column surface is chiral: the tetrameric planes do not pile up in register but are continuously rotated one with respect to the other to generate a chiral column similar to the four-stranded helix formed by poly(G) and by homoguanylic oligodeoxynucleotides.

X-ray Diffraction. In the following, we will refer to the spacing of the observed peaks in values of s ($s = (2 \sin \theta)/\lambda$, where 2θ is the scattering angle and λ the X-ray wavelength).

According to our previous results,[12] all the observed liquid crystalline phases are columnar, as essentially indicated by the characteristic peak centred at *ca.* (3.4 Å)$^{-1}$ in the high-angle X-ray diffraction region. The structural model for these aggregates is similar to that proposed for a dimer of deoxyguanosine[3] and widely confirmed by results obtained in other similar molecular systems:[4-6,21] the columns consist of a stacked array of tetramers formed by Hoogsteen- bonded folate residues, spaced at a distance of about 3.4 Å (see Figure 3).

As a typical example, Figure 4 shows the X-ray diffraction profiles observed in the ternary system $Na_2Fol/NaCl/H_2O$ at 0.50 and 0.28 w/w folate concentrations and recorded at 40 °C. In these two conditions, optical microscopy reveals the presence of a hexagonal and a cholesteric phase, respectively. In both pictures, the high-angle peak due to the stacking of the tetramers and located at $s = (3.4 \text{ Å})^{-1}$ is detected (see the inset), confirming the columnar model described above. In Figure 4a ($c = 0.50$ w/w), two low-angle peaks (orders +1 and −1) of the 2-dimensional hexagonal liquid crystalline phase are easily identified. Using a Guinier camera, we were able to identify higher order reflexions (up to the fifth order in some cases); however, no extra low-angle peaks were observed in this phase, indicating the absence of a smectic-like order. As expected, no long-range column–

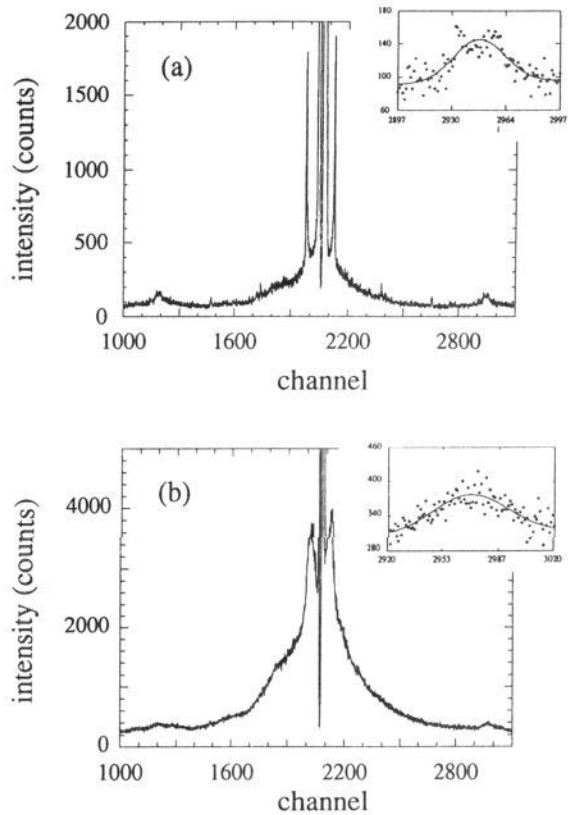

Figure 4. X-ray diffraction profiles of $Na_2Fol/NaCl/H_2O$ at 40 °C in the hexagonal ($c = 0.5$) (a) and cholesteric ($c = 0.28$) (b) phase. The direct beam (centered in a at channel 2037 and in b at channel 2061) is blocked by a beamstop. In the low-angle region, the peaks due to the liquid crystalline order can be observed. The asymmetry is due to smearing effects. In the high-angle region, the peaks reflecting the stacking of the tetramers are located near the maximum of the structure factor of water. The insets in a and b show the diffraction peaks centered respectively at channels 2948 and 2972 ($s = (3.37 \text{ Å})^{-1}$). The solid lines represent the Gaussian fitted to the data. The full widths at half-maximum (fwhm) are 10.0 and 19.4 channels, respectively.

column correlation of the tetramer position exists: the parallel columnar aggregates, formed by piled tetramers and packed in a 2-dimensional hexagonal array, may freely translate in a direction perpendicular to the hexagonal cell.

In Figure 4b ($c = 0.28$ w/w), the X-ray diffraction profile shows broad bands, whose maxima are hardly visible with the resolution obtained with the diffractometer but which were clearly resolved with the Guinier camera. The liquid crystalline phase is assumed to be cholesteric, as confirmed by optical microscopy. In this phase, the columnar aggregates, formed by piled tetramers, are arranged in a helicoidal fashion: the observed low-angle peak corresponds to the mean distance between neighboring cylinders.

The low-angle pattern relative to the hexagonal phase in the Na_2Fol/H_2O system is very sensitive to the concentration: in particular, when the transition to the isotropic phase is approached, the peak becomes more and more broad and diffuse. As the optical microscopy observations exclude the existence of a nematic phase and indicate a direct but very wide hexagonal–isotropic transition, this behavior seems to indicate that dilution establishes a continuous disordering of the hexagonal packing, which eventually leads to the transition. It can also be remarked that some additional weak diffuse scattering is observed in the hexagonal phase at the lower concentration investigated, either in the absence or in the presence of salts.[22]

X-ray diffraction profiles relative to the isotropic phases (not shown) are characterized by the absence of the high-angle peak.

(20) Spada, G. P.; Brigidi, P.; Gottarelli, G. *J. Chem. Soc., Chem. Commun.* **1988**, 953. Gottarelli, G.; Spada, G. P.; Mariani, P.; De Morais, M. M. *Chirality* **1991**, *3*, 227.

(21) Carsughi, F.; Ceretti, M.; Mariani, P. *Eur. Biophys. J.* **1992**, *21*, 155.

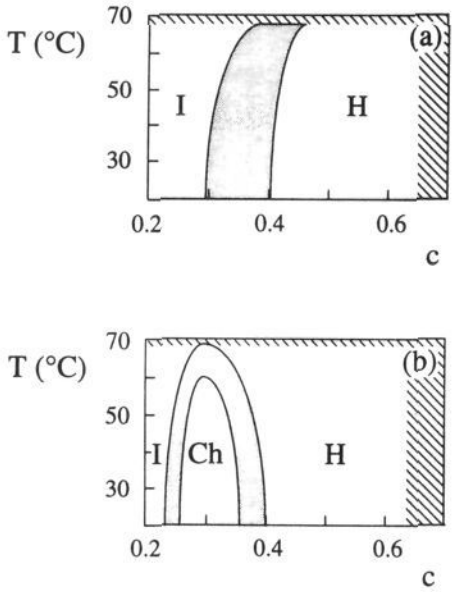

Figure 5. Phase diagrams of Na_2Fol/H_2O (a) and $Na_2Fol/NaCl/H_2O$ with [NaCl] = 1 mol L^{-1} (b) as deduced from X-ray diffraction and optical microscopy measurements. I, Ch, and H refer to isotropic, cholesteric, and hexagonal mesophases, respectively. The shaded areas represent a biphasic region; the hatched areas represent regions for which we have no data.

In Figure 5, the phase diagrams of the binary system Na_2Fol/H_2O and of the ternary system $Na_2Fol/NaCl/H_2O$ are reported. In pure water, the phase sequence previously determined at room temperature is confirmed.[12] It can be noted that the direct isotropic-to-hexagonal phase transition appears to be very wide at all the investigated temperatures. In the phase diagram in 1 mol L^{-1} NaCl, the main difference is the presence of a cholesteric phase, intermediate between the hexagonal and the isotropic phases. However, at high temperature a direct isotropic–hexagonal phase transition is again observed. It is interesting to note that the regions of two-phase coexistence appear to be considerably reduced and that the columnar mesophases extend to a far lower concentration. The general features of these phase diagrams are in agreement with the diagram recently determined[23] for deoxyguanosine 5′-monophosphate in water and in 4 mol L^{-1} KCl as well as with phase diagrams calculated for a hard-particle model[24] or for persistent flexible rods.[25] These theoretical approaches indicate that the stability of columnar phases depends on the properties of the aggregates (such as flexibility and length) and on the aggregation strengths. In particular, in the case of completely rigid aggregates, Taylor and Herzfeld[24] obtain for a weak aggregation (*i.e.*, when the average aggregate size is small) a direct isotropic–hexagonal phase transition with increasing amphiphile concentration, but, for a sufficiently strong aggregation (*i.e.*, when the aggregates are on average sufficiently elongated), they find a stable nematic phase intervening between the isotropic and the columnar phases. Moreover, in the case of persistent flexible long rods, Hentschke and Herzfeld[25] find for moderate flexibility an isotropic–nematic–hexagonal phase sequence with increasing amphiphile concentration; however, as the rods become more flexible, the isotropic–nematic transition recedes to higher concentrations until finally a direct isotropic-to-columnar transition occurs. On the basis of these model phase diagrams, we suggest that NaCl could determine a stronger aggregation of the tetramers, so that cylinders are on average sufficiently elongated to determine the appearance of the nematic phase. The salt could also reduce the flexibility of the columns, thus contributing to stabilizing the nematic phase.

Structural Properties of the Columns

Low-Angle Region of the X-ray Scattering Profile. From X-ray diffraction profiles, the hexagonal unit cell a and the mean distance between adjacent cylinders in the cholesteric phase (in the case of the $Na_2Fol/NaCl/H_2O$ system) have been determined.[26,27]

As reported in detail in ref 23 (see also refs 5 and 28), structural information about the columns could be obtained by analyzing the variation of the dimensions of the hexagonal unit cell a and eventually of the mean distance between the adjacent cylinders in the cholesteric phase as a function of volume concentration, c_v. Assuming that the four-stranded columns in the hexagonal phase are infinitely long and have a circular section with radius R, the relation between the cross sectional area of the rod and the 2-dimensional hexagonal unit cell surface is[4,23,27]

$$\pi R^2 = (\sqrt{3}/2)a^2 c_v \qquad (2)$$

In the present columnar systems, the structure and conformation of the disk-shaped tetramers are not expected to change as a function of the concentration,[8,12,29] so R could be considered constant. Therefore, for infinite cylinders, a will change with volume concentration as:

$$a = (2\pi R^2/\sqrt{3})^{1/2} c_v^{-1/2} \qquad (3)$$

This relationship, $a \propto c_v^{-1/2}$, means that the rods move apart only laterally as dilution proceeds.

By contrast, recent results on some lipid systems[28,30,31] and on deoxyguanosine 5′-monophosphate[23] evidence the presence of finite rods in the hexagonal phase. In this case, in the hexagonal phase the finite cylinders are packed into the 2-dimensional cell with parameter a, but with an average distance C (normal to the hexagonal plane) between cylinder centers. If L is the length of the cylinder, it follows that:

$$L\pi R^2 = C(\sqrt{3}/2)a^2 c_v \qquad (4)$$

Therefore, the variation of the dimension of the hexagonal unit cell with volume concentration depends on the variation of the ratio L/C, *i.e.*, the fraction of water in the C direction. In particular, it has been demonstrated that $a \propto c_v^{-1/3}$ is specific of a situation in which dilution occurs around the finite columns in all three dimensions isotropically.[23,24,28,30]

Moreover, on the basis of theoretical calculations,[24,25] a power law dependence has been predicted for the variation of a with volume concentration for monodisperse spherocylinders of fixed length, with short-range repulsions only. In these calculations, the flexibility of the aggregates plays an important role. The theory distinguishes between spherocylinder length situations

(22) Due to the instrumentation used, we are unable to discuss this diffuse scattering quantitatively. However, several papers, based on high-flux synchrotron radiation experiments, report the observation of diffuse scattering in the X-ray diffraction patterns relative to lyotropic hexagonal phases; this additional diffusion was associated with the fluctuation of the shape of the aggregates or the modulation along the length of the cylinders. See, for example: Rançon, Y.; Charvolin, J. *J. Phys. Chem.* **1988**, *92*, 2646. Rançon, Y.; Charvolin, J. *J. Phys.* **1987**, *48*, 1067. Kékicheff, P.; Cabane, B. *J. Phys.* **1987**, *48*, 1571.

(23) Franz, H.; Ciuchi, F.; Di Nicola, G.; De Morais, M. M.; Mariani, P. *Phys. Rev. E*, in press.

(24) Taylor, M. P.; Herzfeld, J. *Phys. Rev. A* **1991**, *43*, 1892.

(25) Hentschke, R.; Herzfeld, J. *Phys. Rev. A* **1991**, *44*, 1148.

(26) *International Tables for X-ray Crystallography*; The Kynoch Press: Birmingham, U.K., 1952; Vols. 1 and 2.

(27) Luzzati, V. In *Biological Membranes*; Chapman, D., Ed.; Academic Press: London, 1968; Chapter 3.

(28) Amaral, L. Q.; Gulik, A.; Itri, R.; Mariani, P. *Phys. Rev. A* **1992**, *46*, 3548.

(29) Fisk, C. L.; Becker, E. D.; Miles, H. T.; Pinnavaia, T. J. *J. Am. Chem. Soc.* **1982**, *104*, 3307–3314.

(30) Mariani, P.; Amaral, L. Q. *Phys. Rev. E*, in press.

(31) Mariani, P.; Amaral, L. Q.; Saturni, L.; Delacroix, H. *J. Phys.*, in press.

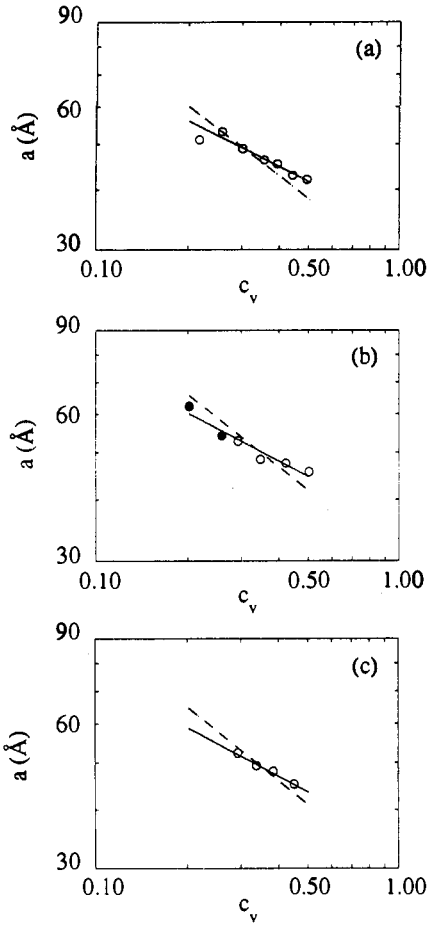

Figure 6. Dimension of the hexagonal unit cell a (○) and distance between columns in the cholesteric phase (●), calculated at 30 °C from the position of the low-angle peaks as a function of the volume concentration, c_v, of folate: (a) Na_2Fol/H_2O; (b) $Na_2Fol/NaCl/H_2O$; (c) $K_2Fol/KCl/H_2O$. The absolute errors on the data for the hexagonal and cholesteric phases are ±1 and ±3 Å, respectively. The straight lines represent fits to the data using the power law with exponent −1/2 (broken) and −1/3 (solid).

relative to a flexibility persistence length.[25,32] In brief, exponents of −1/3 and −1/2 are predicted for spherocylinders that are rigid (shorter than the persistence length) and flexible (longer than the persistence length), respectively. For monodisperse rigid spherocylinders that grow in length with increasing concentration, the theoretical equation for the hexagonal lattice dimension indicates that the exponent will be greater than −1/3.[30]

In Figure 6, we report the a *vs* c_v curves for the Na_2Fol/H_2O, $Na_2Fol/NaCl/H_2O$, and $K_2Fol/KCl/H_2O$ systems at a temperature of 30 °C. The straight lines correspond to −1/2 and −1/3 power law behaviors: it is evident that at all temperatures the data points are alligned well around the curve predicted for finite hard aggregates. However, it must be noticed that the theories discussed above have been derived for the hexagonal phase and that their extension to a cholesteric packing is purely hypothetical. The relevance of these results for the microscopic model of polymorphism is discussed below.

High-Angle Region of the X-ray Scattering Profile. The columnar stacking of the tetramers can be studied in more detail by analyzing the shape and position of the high-angle (s = (3.4 Å)$^{-1}$) peak. As previously observed for folate at room temperature[12] and in contrast with the results for the guanosine derivatives investigated,[3,4,6] it can be observed first that dilution strongly modifies the characteristics of the peak either in the presence or in the absence of NaCl. In order to extract information, we fitted a Gaussian and a locally linear background to every peak

(32) Hentschke, R. *Liq. Cryst.* **1991**, *10*, 691.

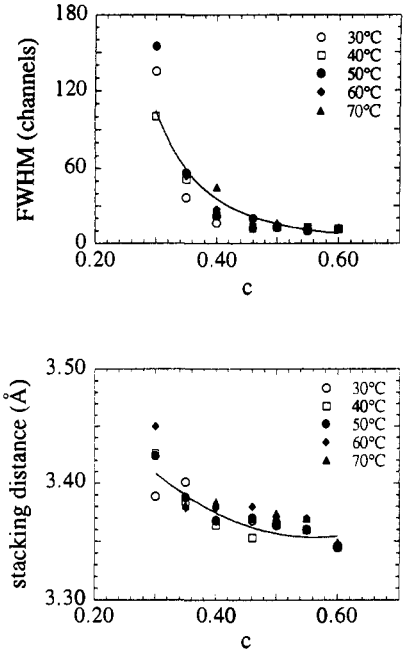

Figure 7. Na_2Fol/H_2O system. Upper frame: full widths at half-maximum (fwhm) of the high-angle peak *vs* folate concentration for different temperatures. Error bars, omitted for clarity, are around 5%. Lower frame: tetramer stacking distance *vs* concentration for different temperatures. Error bars, omitted for clarity, are around 0.01 Å. In both frames, the lines reported are guides to the eyes to show the general trend.

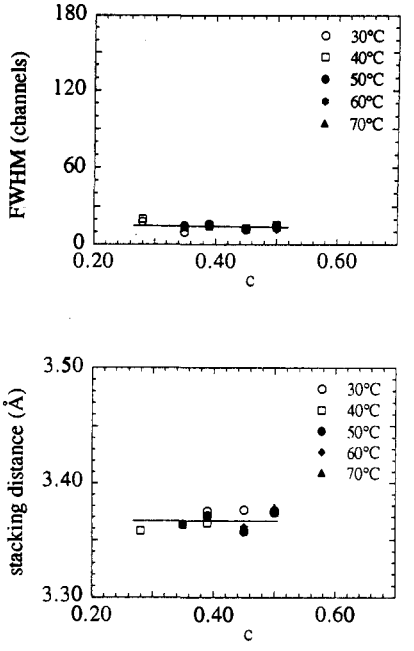

Figure 8. $Na_2Fol/NaCl/H_2O$ system. Upper frame: full widths at half-maximum (fwhm) of the high-angle peak *vs* folate concentration for different temperatures. Error bars, omitted for clarity, are around 5%. Lower frame: tetramer stacking distance *vs* concentration for different temperatures. Error bars, omitted for clarity, are around 0.01 Å. In both frames, the lines reported are guides to the eyes to show the general trend.

(see the inset of Figure 4). The results are summarized in Figures 7 and 8, where data relative to Na_2Fol/H_2O and $Na_2Fol/NaCl/H_2O$ are reported, respectively. In pure water, the distance between the stacked tetrameric disks increases as a function of water content and as a function of temperature. At the same time, the width of the peak also continuously increases as a function of the water content: in particular, the peak becomes very wide for the highest water concentration investigated. The effect of

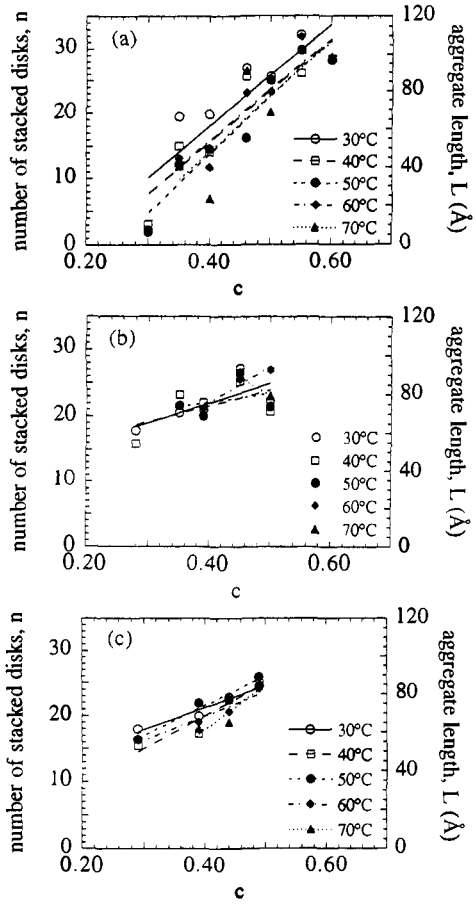

Figure 9. Average number of stacked disks, n, determined by comparing the measured fwhm of the high-angle diffraction peak to the simulated peak width (see text), as a function of folate concentration for different temperatures: (a) Na_2Fol/H_2O; (b) $Na_2Fol/NaCl/H_2O$; (c) $K_2Fol/KCl/H_2O$. The absolute error is ±5. The lines are linear fits to the data to show the general trend. The right-hand side scale is the average columnar length calculated by multiplying n by the stacking distance.

temperature on the peak width in contrast is negligible. In the case of Na_2Fol in 1 mol L^{-1} NaCl solution, the structural behavior is practically the opposite: the stacking distance between the disks remains almost constant as a function of the dilution, and the width of the peak remains practically constant. Moreover, there is in both cases a negligible effect due to changes in temperature.

To correlate the peak width with the average number of stacked tetramers, numerical simulations of the scattering profile for the columnar aggregates were performed. In particular, the tetramers were approximated by homogeneous disks with a thickness of 2.35 Å and a radius of 15.5 Å.[12] The scattering amplitude of a given number n of these disks, stacked one on top of the other at a distance of 3.4 Å, was summed, squared, and then averaged over all orientations. A random fluctuation of the repeat distance could be accounted for: in fact, as expected, this type of disorder has no influence on the width of the diffraction peaks. Moreover, the result is rather insensitive to the radius value used. This procedure is correct as long as there is no 3-dimensional correlation between the positions of the tetramers in the different aggregates (for more details, see ref 23). The average number n of stacked discs forming one column was subsequently determined by comparing the calculated and measured peak widths.

The average correlation lengths of the columnar aggregates obtained by multiplying the number n by the experimental stacking repeat distance are reported as a function of the concentration (and temperature) in Figure 9. It is evident that in the Na_2Fol/H_2O system, the average correlation length of the aggregates changes only slightly as a function of temperature, while it increases continuously as a function of the concentration from *ca.* 15 Å (corresponding to about five piled disks) to 100 Å (about 30 disks). By contrast, in the case of the $Na_2Fol/NaCl/H_2O$ system, the aggregate size is fairly constant as a function of both concentration and temperature: the average aggregate length is around 85 Å (about 25 disks) and slowly decreases when the water content increases (at the cholesteric-to-isotropic phase transition, the average length of the aggregates is *ca.* 65 Å, *i.e.*, about 20 disks).

It may be noticed that the value of n (and thus of the correlation length) determined in this way is an average value, because some polydispersity has to be expected in this system. However, considering the degree of experimental accuracy, the polydispersity does not need to be treated in a quantitative manner. At all concentrations and temperatures investigated, the observed peaks could be perfectly fitted with a single Gaussian, indicating that the polydispersity is rather small and the length distribution symmetric. From the aggregate average length and the corresponding unit cell dimension, the end-to-end distance between two aggregates, Δ, can be derived. In fact, from eq 4 and using $C = (L + \Delta)$, it follows

$$\Delta = L[-1 + 2\pi R^2/(\sqrt{3}c_v a^2)] \qquad (5)$$

The end-to-end distances calculated for the three investigated systems are reported in Figure 10. While L has been directly determined from the high-angle X-ray diffraction peak, the absolute value of Δ is strongly dependent on the value of R used, which can only be estimated from molecular models and from previous results.[8,12,29] In the case of folate in pure water, the end-to-end distance increases only sligthly (from about 15 to 20 Å) as a function of the water content and appears to be quite independent of the temperature. By contrast, in the system containing NaCl, Δ increases continuously (from about 15 to 35 Å) as a function of the water content. In this case, the dependence on the temperature is more clear: when the temperature rises, the end-to-end distance increases. It should be noted that the data relative to the lowest concentrations do not follow the general trend: in fact, in both cases of folate in pure water or in 1 mol L^{-1} NaCl, samples are in the two-phase region, so that the phase concentration may not correspond to the sample composition. Note also that this end-to-end distance should not be regarded as the thickness of a water layer as occurs in a smectic phase, because there is no correlation between the position of the columns in the axial direction. The absence of X-ray diffraction associated with the finite dimension of the cylinders could also be ascribed to the polydispersity of their lengths.[23,28]

Discussion

In the previous sections we have reported and discussed in detail several characteristics of the liquid crystalline state, namely: (i) the presence or the absence of the cholesteric phase in the phase diagram; (ii) the effect of dilution on the lateral and vertical distances between the columnar aggregates, as deduced from the low-angle diffraction, and the relative implications in terms of rigidity and dimensions of the columns; and (iii) the effect of dilution and temperature on the shape and position of the high-angle peak in relation to the distance between the tetrameric disks. From this study, information is obtained on the number of disks in the columns and again on the columnar end-to-end distances.

An inspection of all these data gives a rather detailed picture of the self-assembly process of folates and of the effect of ions.

In all the investigated temperature ranges, folate in pure water does not exhibit a cholesteric phase. The interactions between the piled tetramers are weak, as indicated by the unusual increase of the stacking repeat distance and by the decrease of the average number of stacked tetramers per column, as a function both of

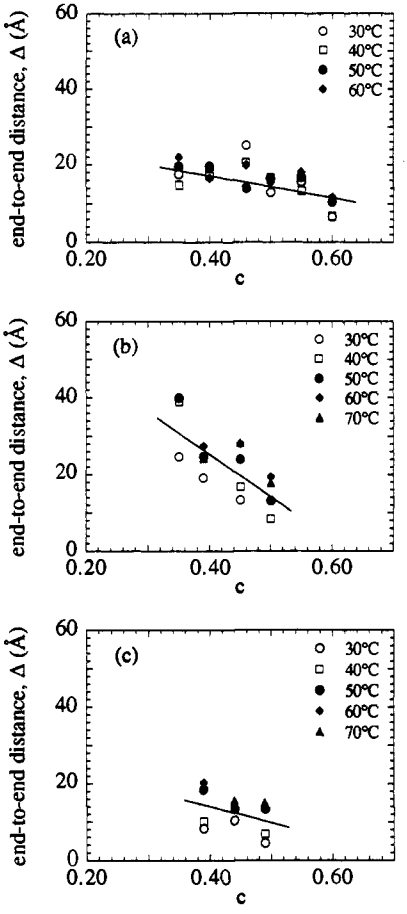

Figure 10. Axial end-to-end distance Δ between cylinders in the hexagonal phase *vs* folate concentration for different temperatures: (a) Na_2Fol/H_2O; (b) $Na_2Fol/NaCl/H_2O$; (c) $K_2Fol/KCl/H_2O$. The absolute error is estimated to be ±10 Å. The lines reported are guides to the eyes to show the general trend. Data relative to concentrations equal to and lower than 0.3 are not reported, as samples are in the two-phase region and therefore the phase concentration may not correspond to the sample composition. Moreover, in the case of Na_2Fol/H_2O (frame a), data at 70 °C are not reported, as they appear largely affected by uncontrollable sample inhomogeneity, which became more evident as the concentration fell below 0.5.

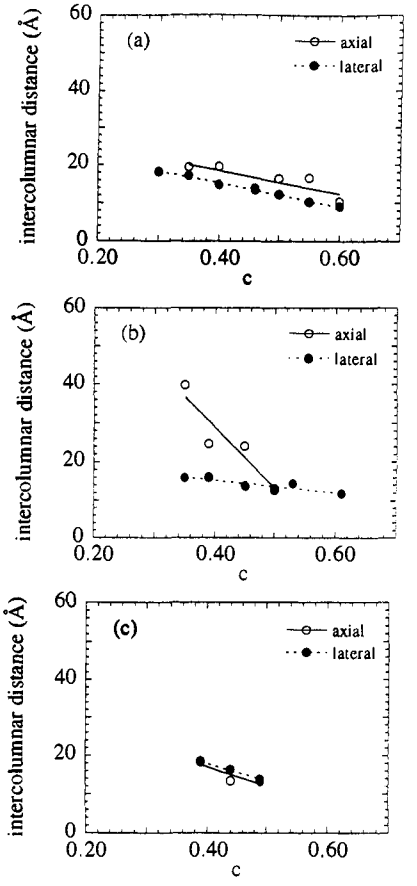

Figure 11. Axial and lateral distances between cylinders in the hexagonal phase *vs* folate concentration at 50 °C: (a) Na_2Fol/H_2O; (b) $Na_2Fol/NaCl/H_2O$; (c) $K_2Fol/KCl/H_2O$. The absolute error is estimated to be ±3 and ±10 Å for the lateral and axial distances, respectively. The lines reported are guides to the eyes to show the general trend.

temperature and of water concentration. The strong sensitivity of the columnar length to the concentration is remarkable: in particular, close to the isotropic–hexagonal phase transition, the columns are formed by only five disks (Figure 9). This finding explains, on the one side, the disordering of the hexagonal phase, observed when the water concentration increases, as deduced from the reduction of intensity and the broadening of the low-angle diffraction peaks. On the other side, this fact is in complete agreement with the SANS results: in the isotropic phase, due to the weak tetramer interactions, even at concentrations of 0.04 w/w and at a temperature of 10 °C, no scattering particles were detected.[13]

Therefore, as a function of the water content, the length of the columns continuously decreases, while, at the same time, the column end-to-end distance increases only slightly. These results can be compared to the effect of water addition on the *a* parameter in the hexagonal phase. At all concentrations, we observe that the lateral distance between nearest neighboring columns (see Figure 11), defined as $(a - 2R)$, and the intercolumnar end-to-end axial distance (Δ) are roughly comparable. The water addition affects mainly the length of the aggregates and moves the columns apart both laterally and axially in a quasiisotropic way.

All these data are compatible with a model of rigid and reversibly assembled rodlike aggregates, with average size (length) increasing with increasing concentration and with decreasing temperature. According to Taylor and Herzfeld,[24] the absence of a cholesteric phase can be explained as follows:[6] as the aggregation is weak, *i.e.*, as at the transition the average aggregate size is small (the aggregates are essentially spheroidal), the cholesteric phase is unstable and a direct isotropic-to-hexagonal phase transition is observed.

The first effect obtained after addition of NaCl is the appearance of the cholesteric phase. On the basis of the approach developed by Taylor and Herzfeld,[24] a stable nematic phase intervening between the isotropic and the hexagonal phases can be found when finite rigid aggregates are on average sufficiently elongated. Moreover theoretical calculations show that nematic phases may also become stable due to a decrease of flexibility of long aggregates.[24,25,32] In both cases, the existence of the cholesteric phase is determined by a sufficiently strong aggregation.

All structural data are consistent with these hypotheses. On the one side, the stronger tetramer interactions induced by NaCl are confirmed by the constancy of the stacking repeat distance, as a function of both the temperature and the concentration, and of the aggregate length as a function of temperature. As a function of the water content, the length of the columns decreases only slightly. Therefore, at the transition, the rods are sufficiently elongated and rigid that the cholesteric phase is stable.

The stability of the cholesteric phase is also influenced by the end-to end distance. In the case of folate in 1 mol L^{-1} NaCl, the axial intercolumnar separation increases as a function of temperature. Therefore, the reduction of the cholesteric domain observed at high temperature can be explained: even if the aggregate length is not sensitive to temperature and flexibility

does not appear to change, the continuous increase of the end-to-end distance as a function of temperature could determine a very loose packing of the hexagonal phase so that a direct hexagonal-to-isotropic phase transition appears (see also ref 5).

As reported above, the addition of NaCl determines a stabilization of the columns, related to a stronger interaction between the stacked tetramers. As a result, columns with lengths roughly independent of concentration are formed. With respect to folate in pure water, this stabilization is also accompanied by an increase in the 2-dimensional hexagonal lattice dimension: the addition of water increases both lateral and axial columnar distances, as expected considering the exponent of $-1/3$ observed in the a *vs* c_v curves.[28,30] However, with respect to the changes in the lateral distance between nearest neighboring columns (comparable to what was observed for samples in pure water), the intercolumnar end-to-end axial distance increases rapidly with water content.

The observation that the aggregate length slowly decreases when the water content increases has another consequence. By contrast with the results obtained with folate in pure water, scattering particles have been detected in 1 mol L^{-1} NaCl at the concentration of 0.04 w/w by SANS measurements:[13] the scattering curves are compatible with the presence of short aggregates formed by nine piled disks; nine is also the average number of stacked tetramers per column, which is determined by linear extrapolation of the data relative to the length of the columns in the liquid crystalline phases reported as a function of the concentration.

The stronger tetramer interactions determined in 1 mol L^{-1} NaCl may be attributed to a specific interaction of Na^+ ions, which have the right size to keep together two tetrameric planes *via* coordination with the eight oxygens of the folate residues. The subsequent effect is the observed constancy of the tetramer stacking distance and of the aggregate length with temperature and concentration. The columns are rigid aggregates; therefore, the addition of water will increase the volume around the particles in all three dimensions.

The addition of KCl is not associated with the formation of a stable cholesteric phase; this could be observed by microscopy only as a transient species by rapid evaporation of a diluted solution. The X-ray data for the hexagonal phase are similar to those obtained in the presence of NaCl (Figures 10 and 11), with the exception of the end-to-end axial distances, which are more similar to those in pure water. The overall situation in KCl seems to be intermediate between those in pure water and in NaCl. A similar picture is obtained also in isotropic solutions[13] by SANS, CD, and ^{1}H-NMR spectroscopy.

It should be noticed that, while in guanosine derivatives K^+ favors the assembling process better than Na^+, folates are better assembled by Na^+ ions. The small geometrical differences between guanine and pterin could be related to this inversion of selectivity.

Experimental Section

Disodium and dipotassium folate were prepared by neutralization of folic acid (dihydrate, from Sigma) with sodium hydroxide and potassium hydroxide, respectively. The weighted solutions were left for at least 2 days at room temperature to avoid inhomogeneity. The homogeneity of the samples was verified by optical polarizing microscopy. The relative uncertainty of the concentrations was estimated to be 0.03 w/w. Concentrations are reported as weight/weight (c) or volume concentration (c_v) as appropriate. The volume concentration was calculated using for Na_2Fol the specific volume 0.651 cm^3/g.

Optical Microscopy. Microscopic observations were carried out with a Zeiss polarizing microscope equipped with a photocamera. Preliminary observations were made on samples with peripheral evaporation. Cholesteric solutions were inserted into rectangular capillaries (thickness 0.3 mm, from Vitrodymamics), sealed with wax; the samples were then oriented by putting them into a 0.5-T magnet for *ca.* 5 h.

X-ray Diffraction. Low-angle X-ray diffraction experiments were performed using a 1.5-kW Ital-Structures X-ray generator equipped with a Guinier-type focusing camera operating in vacuum: a bent quartz crystal monochromator was used to select the Cu $K\alpha_1$ radiation (λ = 1.54 Å). The samples were mounted in vacuum-tight cells with thin mica windows. In order to reduce the spottiness arising from possible macroscopic monodomains, the cells were continuously rotated during the exposure. The sample cell temperature was controlled with an accuracy of 0.5 °C by using a circulating thermostat. The diffraction patterns were recorded on a stack of four Kodak DEF-392 films. Scattering data were also recorded on a two- circle diffractometer equipped with a bent position-sensitive detector (INEL CPS120) to record the scattered intensity in a range of $\Delta 2\theta = 120°$ at the same time. A Philips PW1830 was used as X-ray source, run at a power of 1.6 kW with a copper target. The Cu $K\alpha_1$ line was selected by a monochromator focused on the detector. The intrinsic resolution of the diffractometer (width of a crystalline peak) was determined to be 1.1 channels. The width of one channel was measured using a LiF single crystal and calculated to be 0.0300(2)°.

Circular Dichroism. CD experiments were performed with a Jasco J710 spectropolarimeter on cholesteric solution inserted into a 0.001-cm path length cell. The planar orientation of the cholesteric mesophase was obtained utilizing the surface effect of the cell walls. The alignment was checked by polarizing microscopy.

Acknowledgment. H.F. would like to acknowledge the support of the European Economic Community under contract no. ERBCHBGCT920204. This work was partially financied by MURST and CNR (Italy). G.G. and G.P.S. thank Ms. Stefania Zanella for technical assistance.